Magnetic and magnetotransport properties of Fe-based glass-covered microwires

2004 J. Phys.: Condens. Matter 16 6279

(http://iopscience.iop.org/0953-8984/16/34/025)

INSTITUTE OF PHYSICS PUBLISHING JOURNAL OF PHYSICS: CONDENSED MATTER

J. Phys.: Condens. Matter **16** (2004) 6279–6291 PII: S0953-8984(04)77737-1

Magnetic and magnetotransport properties of Fe-based glass-covered microwires

Marco Coïsson, Paola Tiberto and Franco Vinai

IEN Galileo Ferraris, strada delle Cacce 91, I-10135 Torino, Italy

E-mail: coisson@ien.it

Received 10 March 2004
Published 16 August 2004
Online at stacks.iop.org/JPhysCM/16/6279
doi:10.1088/0953-8984/16/34/025

Abstract

Magnetic and magnetotransport properties of glass-covered amorphous microwires of nominal composition $Fe_{89}B_1Si_3C_3Mn_4$ have been studied. Samples of two families with the same composition but different metallic core diameters were annealed in a furnace or by Joule heating. The electrical resistance was measured as a function of time during annealing to study the effects on the samples' microstructures (evolution from the amorphous to the crystalline phase). Static hysteresis loops were measured on all samples by means of a vibrating sample magnetometer. Giant magneto-impedance measurements (GMI) performed on a coaxial line using a vectorial network analyser at frequencies up to 6 GHz showed that furnace-annealed samples display larger anisotropies with respect to Joule-heated ones; however, Joule heating is more effective in improving the magneto-impedance response of the alloy. The maximum GMI ratio is $\approx 175\%$ at 4 GHz. The influence of the different metallic core/total wire diameter on the induced anisotropies has been studied for the two families of samples through hysteresis loops and high-frequency GMI.

1. Introduction

In the last decade many experimental and theoretical papers have investigated the giant magneto-impedance (GMI) phenomenon on amorphous magnetic materials [1–4]. This effect consists in a large electrical impedance variation of a magnetic sample when submitted to a static magnetic field; it can be either parallel or perpendicular to the direction of the current used for measuring the impedance. In a common configuration (the one used here), the ac impedance of a magnetic wire or ribbon is measured through its length; the dc magnetic field is applied along the sample axis and plays the role of modifying the sample domain configuration. The ac current used for measuring the impedance generates an ac magnetic field (circular for wires, transversal for ribbons) that causes the domain wall oscillation around

the equilibrium position given by the minimization of all energy terms, including the one due to the applied static field. This movement of the domain walls can be described in terms of circular or transversal magnetic permeability [5], which is a function of the domain configuration and thus of the applied static magnetic field, and is responsible for a contribution to the total electrical impedance of the magnetic sample. As a consequence, by applying a static magnetic field along the axis of the sample an impedance variation is obtained.

Generally, large impedance variations are typically observed in Co-based amorphous alloys with nearly zero magnetostriction, both in wire and ribbon form [6], although some Fe-based compositions have shown some GMI effect (small when compared with Co-based alloys) [7].

Conventionally, GMI is measured up to an exciting current frequency of a few MHz, where the four-point technique is applicable. For relatively small samples, if an impedance analyser is used, the frequency of the current used for measuring the impedance can be raised from a few tens up to a few hundreds of MHz [8, 9]. In the last few years many techniques have been employed making use of network analysers to investigate higher frequencies (up to a few GHz). Most of them measure the scattering parameters of a coaxial line whose inner conductor is the magnetic material [10–13]. Independent of the details of the applied technique, a widely used configuration is a coaxial line whose inner conductor is the magnetic sample; the magnetic field that propagates is circular and the applied static magnetic field is parallel to the axis direction, thus preserving the geometry of the conventional GMI measurements. After a proper characterization of the transmission line (that depends on the details of the experimental technique used), a quantity directly related to the magnetic properties of the sample can be obtained, for example the characteristic impedance of the line [11]. Its variation as a function of the applied static magnetic field is called (high-frequency) GMI.

This high-frequency study has both theoretical and practical interest. It has been shown that high-frequency GMI is directly related to the circular magnetic permeability in Co-based microwires [12] and provides an alternative technique to study ferromagnetic resonance [14] (and also properties such as saturation or anisotropies of the magnetic sample). For this reason, high-frequency GMI can give important clues on how anisotropies, shape, permeability and overall domain configuration determine the complex behaviour of a magnetic material at frequencies in the GHz region. From a practical point of view, large GMI ratios at microwave frequencies can be useful in the design of sensors or integrated devices that operate at a frequency of a few GHz.

This paper reports a large set of experimental results on two families of magnetic glass-coated microwires of nominal composition $Fe_{89}B_1Si_3C_3Mn_4$. In spite of their being an Fe-based alloy, impedance variations as high as 150% at 4 GHz have already been observed [15]. In addition to high-frequency GMI results, samples of the studied composition have been submitted to thermal treatments (both furnace annealing and Joule heating), in order to modify their domain structure and anisotropies; static longitudinal hysteresis loops and GMI responses have been measured on all treated samples. This systematic study has been performed to collect a large set of data in an attempt to put into evidence the relationship between magnetic and magnetotransport properties that lead to such surprisingly high GMI ratios in this alloy.

2. Experimental setup

Amorphous microwires of nominal composition $Fe_{89}B_1Si_3C_3Mn_4$ have been produced by means of the glass extraction technique [16–18]. Samples of two families have been obtained: thick wires (metallic diameter $\approx 10\,\mu$m) and thin wires (metallic diameter $\approx 5\,\mu$m); in both cases, the glass coating has a thickness of about $5\,\mu$m.

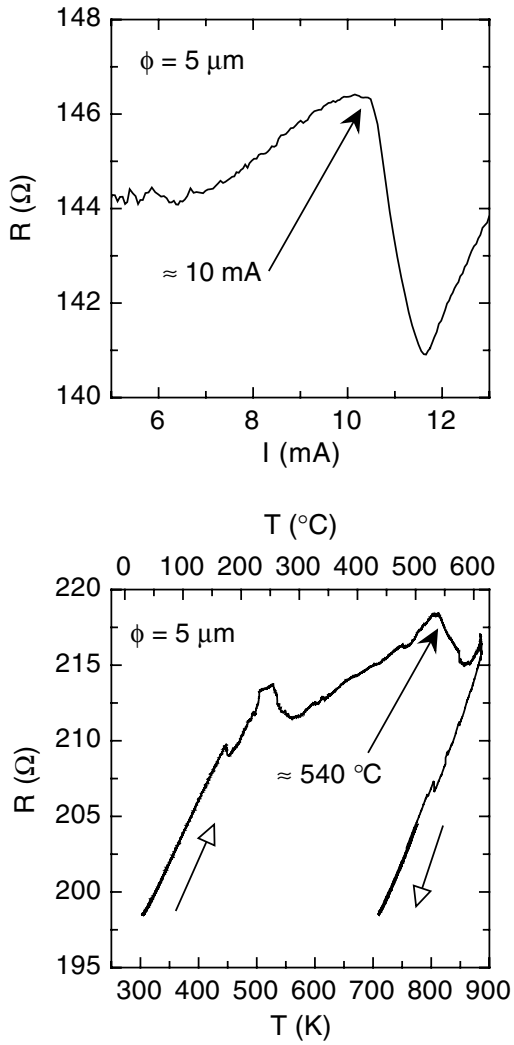

Figure 1. Upper panel: resistance versus annealing current for Joule-heated thin microwires. Lower panel: resistance versus annealing temperature for furnace-annealed thin microwires.

Selected samples of both families have been submitted to thermal treatments, both furnace annealing (for 1 h) and Joule heating (for 1200 s); the latter is a current-annealing technique under a self-generated circular magnetic field. To determine the crystallization current and the crystallization temperature of both thick and thin wires, selected samples have been submitted to temperature ramps in furnace or to heating current ramps for Joule heating. In all cases, the electrical resistance has been monitored as a function of temperature or current; it being a structure-sensitive property enables the detection of structural variations (e.g. stress relaxations or crystallization) in the sample [19]. Figure 1 reports the data on Joule-heated and furnace-annealed thin samples: for Joule heating the resistance remains initially constant, then increases as an effect of the heating of the sample. As expected, the onset of crystallization is marked by a huge drop in the electrical resistance. After the crystallization process has been completed, the resistance starts increasing again as an effect of the heating process. A similar discussion

Table 1. Thermal treatments (furnace annealing and Joule heating) applied to the studied thick and thin amorphous microwires.

Family	Furnace annealing (°C, 1 h)	Joule heating (mA, 1200 s)
Thick wires	350, 450, 500	5, 7, 10, 12, 15, 17
Thin wires	400, 450, 500, 550	5, 7, 9

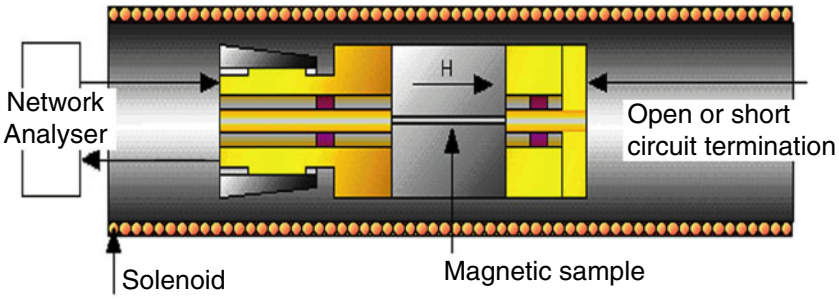

Figure 2. Coaxial line used for GMI measurements. The magnetic sample is the inner conductor. The solenoid generates the static longitudinal field. The termination cap a provides a short-circuit termination and, if removed, an open-circuit termination is obtained.

(This figure is in colour only in the electronic version.)

is applicable to furnace-annealed wires, although the resistance immediately starts increasing just above room temperature. Thick and thin samples are characterized by a crystallization temperature of about 510 and 540 °C respectively; their crystallization currents were about 25 and 10 mA respectively. Given these results, selected samples have been submitted to the thermal treatments summarized in table 1.

High-frequency GMI [11] has been measured on all thermally treated as well as as-prepared samples. The characteristic impedance Z_0 of the coaxial line containing the magnetic sample is obtained through a double measurement of the reflection parameter S_{11} of the coaxial line (shown in figure 2). The measurement cell is terminated with an open circuit or a short circuit, and the total impedance Z_i (with $i = open$ or $short$) is calculated as $50(1 + S_{11})/(1 - S_{11})$, where 50 is the characteristic impedance (in ohms) of the network analyser connectors and cables. Once both impedances Z_{open} and Z_{short} have been measured, the characteristic impedance of the line can be calculated as follows:

$$Z_0^2 = \frac{Z_{Lopen}Z_{Lshort}(Z_{open} - Z_{short})}{(Z_{open} - Z_{short}) - (Z_{Lopen} - Z_{Lshort})} - \frac{Z_{open}Z_{short}(Z_{Lopen} - Z_{Lshort})}{(Z_{open} - Z_{short}) - (Z_{Lopen} - Z_{Lshort})}, \quad (1)$$

where Z_{Lopen} and Z_{Lshort} are a proper model for the open and short circuit terminations. Once the characteristic impedance Z_0 is determined for each desired frequency and each desired value of the static longitudinal magnetic field (whose maximum value H_{max} is equal to 40 000 A m^{-1} in our case), the GMI ratio (%) is defined as

$$\frac{\Delta Z_0}{Z_0} = \frac{Z(H) - Z(H_{max})}{Z(H_{max})}100. \quad (2)$$

Longitudinal static hysteresis loops have also been measured by means of a vibrating sample magnetometer (maximum applied magnetic field = 10 kA m^{-1}).

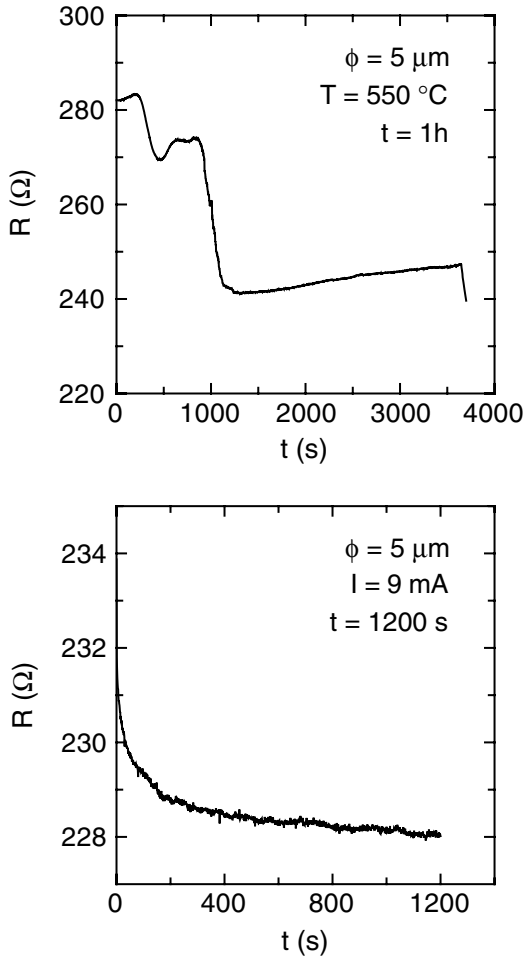

Figure 3. Upper panel: resistance versus time for a furnace-annealed thin microwire. Lower panel: resistance versus time for a Joule-heated thin microwire.

3. Results and discussion

In figure 3, resistance versus time curves are given for a thin wire annealed in a furnace (upper panel) and submitted to Joule heating (lower panel); thick samples display similar behaviour. The furnace-annealed wire shows an initial increase in its resistance, due to the temperature increase; then the resistance drops because of possible stress relaxations due to the heating process; then, a larger resistance drop marks the onset of crystallization. After crystallization is complete, the resistance increases again, although slightly, because of the temperature increase of the sample, following the alloy TCR (temperature coefficient of resistance, which indicates how the electrical resistance evolves with temperature for a specific alloy) [19]. This example is provided for a sample annealed at a high temperature, where the crystallization occurs; samples annealed at lower temperatures, where no crystallization features are observed, may only show an increase in the initial resistance or the resistance variation due to relaxation processes. In contrast, Joule-heated samples do not show significant resistance variations

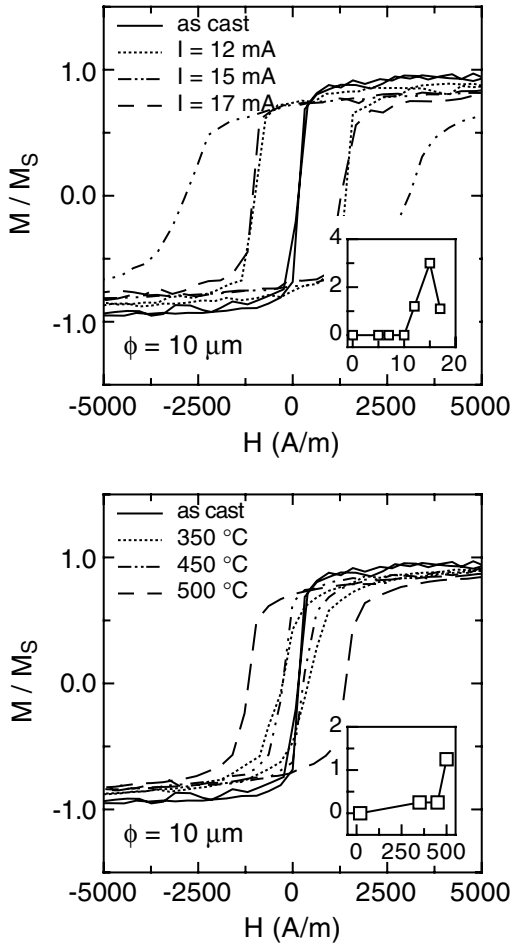

Figure 4. Static longitudinal hysteresis loops for as-prepared and Joule-heated thick wires (upper panel) and as-prepared and furnace-annealed thick wires (lower panel). The insets show the coercive field (kA m^{-1}) as a function of annealing current (mA) (upper panel) and as a function of the annealing temperature (°C) (lower panel).

until crystallization occurs; in this case, as shown in figure 3, the resistance decreases as a function of time. In any case, a circular anisotropy may be induced by the annealing current [20].

Static longitudinal hysteresis loops have been measured for all samples in order to investigate the effect of the structural modifications induced by thermal treatments. Since the mass of the magnetic core of the sample submitted to measurements cannot be known without a very large uncertainty, magnetization curves have been normalized to the saturation value. Hysteresis loops for as-prepared and annealed thick samples are shown in figure 4 and for thin samples in figure 5. All the insets show the coercive field as a function of the annealing current or temperature, as appropriate. The hysteresis loops of Joule-heated thick wires are almost coincident with the one for the as-prepared sample for annealing current values up to 10 mA (the current at which the maximum GMI ratio is observed). Then the coercive field H_C increases. Very strong heating processes (current equal to 17 mA) cause

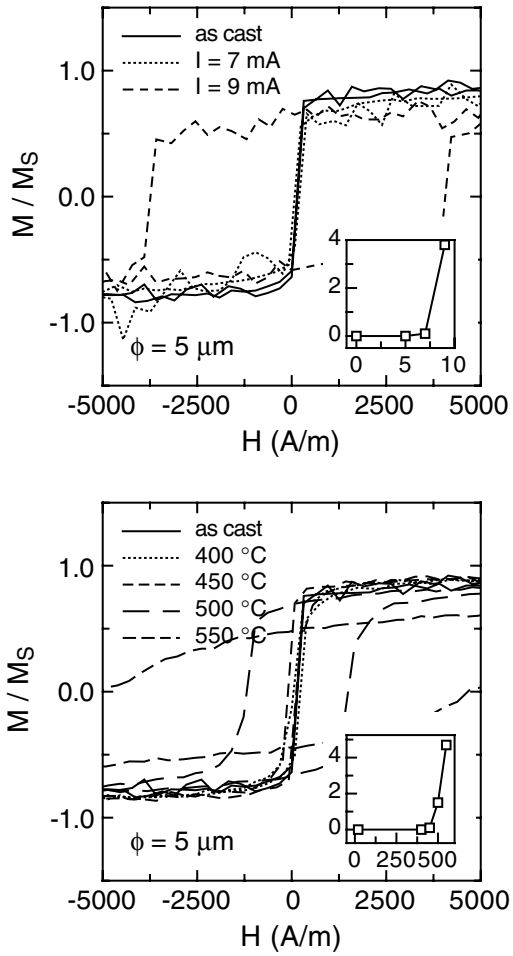

Figure 5. Static longitudinal hysteresis loops for as-prepared and Joule-heated thin wires (upper panel) and as-prepared and furnace-annealed thin wires (lower panel). The insets show the coercive field ($kA\,m^{-1}$) as a function of annealing current (mA) (upper panel) and as a function of the annealing temperature (°C) (lower panel).

a reduction of the coercive field. In contrast, furnace annealing progressively increases H_C. In magnetic materials, the field at which magnetic saturation is reached is given by the ratio of two times the anisotropy constant of the material over saturation magnetization [21]. If the hysteresis loop is sufficiently 'square', the coercive field is approximately equal to this saturation field. In our case, H_C almost always only slightly underestimates the saturation field, so the increase of the coercive field upon annealing can be ascribed to an increase of the total magnetic anisotropy in the sample. From the data in the insets of figures 4 and 5 it is clear that both Joule heating and furnace annealing induce anisotropies in the samples, resulting in large variations of the coercive field. Similar results are obtained for thin wires, except for the fact that no hysteresis reduction is observed in strongly annealed Joule-heated wires.

Although Joule heating is a commonly employed technique for the induction of circular anisotropies in wires [20, 22], in our case furnace annealing seems to be at least equally effective

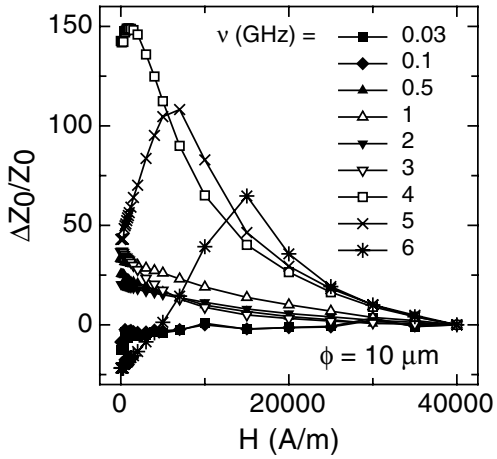

Figure 6. High-frequency GMI curves at selected frequencies for the thick wire Joule-heated at 10 mA for 1200 s.

in inducing anisotropies in the samples; this fact may be accounted for by considering that the studied alloy is mostly composed of iron. Fe-based amorphous materials display a positive magnetostriction constant (for the studied alloy it should be $\approx 40 \times 10^{-6}$), compared with the nearly zero magnetostriction constant of the Co-based alloys that usually display larger GMI ratios. In fact, it is known that magnetostriction has an important influence on the GMI response of a magnetic material [23]. During annealing and especially during cooling down to room temperature, the different thermal expansion coefficients of the metallic core and of the glass coating may induce stresses in the wires [18] that induce radial anisotropies in the alloy [24], because of the relatively large magnetostriction constant. This mechanism is more effective during furnace annealing, where both the metallic core and the glass coating are kept at the same temperature, than for Joule heating, where the current flowing in the sample heats the metallic core more efficiently than the glass coating; even though the circular field generated by the annealing current should induce a circular anisotropy, this may not be effective because of the radial domain structure observed in Fe-based microwires [24], opposed to the circular domain structure of Co-based microwires. In contrast, the stress-induced anisotropy during cooling down in furnace and due to the difference in the expansion coefficients and to the large and positive magnetostriction constant may account for the large increase of H_C observed in furnace-annealed samples. The presence of this radial anisotropy can account for the increasingly slower approach to magnetic saturation that all furnace-annealed samples display with respect to the as-prepared wire. In contrast, Joule heating probably affects hysteresis loops only when the current flowing through the sample is sufficiently high to also start heating the glass coating, thus inducing effects similar to those observed on furnace-annealed samples.

High frequency GMI curves at selected frequencies are shown in figure 6 for one thick sample (Joule heated at 10 mA for 1200 s). Even if the GMI ratio at frequencies up to 3 GHz is already remarkable (always larger than 20%), only at frequencies $\geqslant 4$ GHz does the GMI response become really large (as high as 150% at 4 GHz for this sample). It should be noted that the GMI ratios at these high frequencies are even slightly underestimated, because the maximum applied static field is not sufficient to completely saturate the effect. Since (2) is normalized to the impedance value at H_{max}, if the curve is not yet saturated, the GMI ratio is underestimated; larger static field values would be necessary at frequencies $\geqslant 4$ GHz for a more

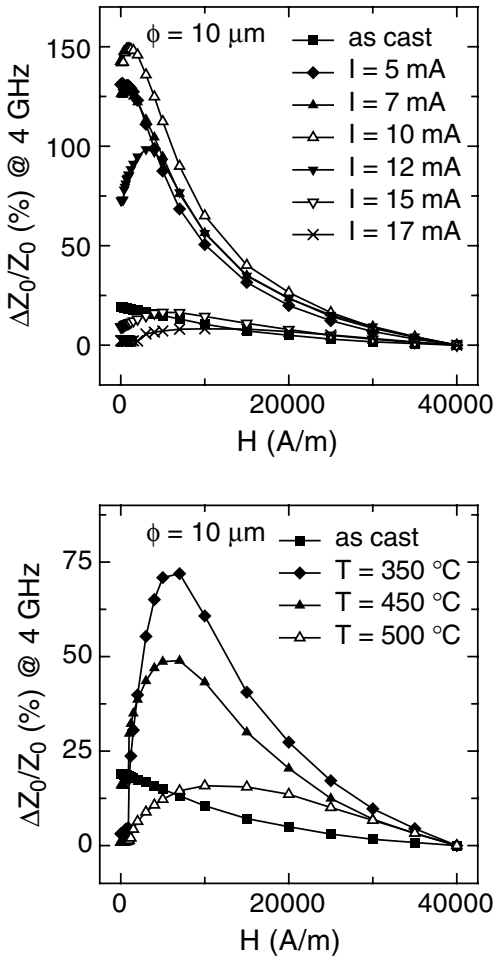

Figure 7. High-frequency GMI curves at a frequency of 4 GHz for as-prepared and annealed thick wires (upper panel: as-prepared and Joule-heated samples; lower panel: as-prepared and furnace-annealed samples).

accurate determination of the GMI response. In spite of this slight underestimation, the GMI effect on these Fe-based microwires is always very large, especially at the highest frequencies. As a function of frequency, the shape of the GMI curves evolves from one peak (monotonically decreasing behaviour from 0 to H_{max}) to two peaks (the GMI ratio increases, then reaches a maximum, then decreases). This is a general feature: when the exciting frequency is low, a one-peak behaviour may be observed even if the sample has large magnetic anisotropies quenched in; then, on increasing the frequency, GMI starts to be more affected by the anisotropy of the sample and when frequencies are of the order of a few GHz, GMI evolves into ferromagnetic resonance; the two-peak curve shapes evolve and the shift towards higher fields of the maximum GMI ratio can be described within this framework [14].

The GMI response is also influenced by the thermal treatments applied to the sample, as shown in figure 7 for thick wires and in figure 8 for thin wires, where $\Delta Z_0/Z_0$ at 4 GHz is reported for all the as-prepared and annealed samples. It can be observed that the best GMI

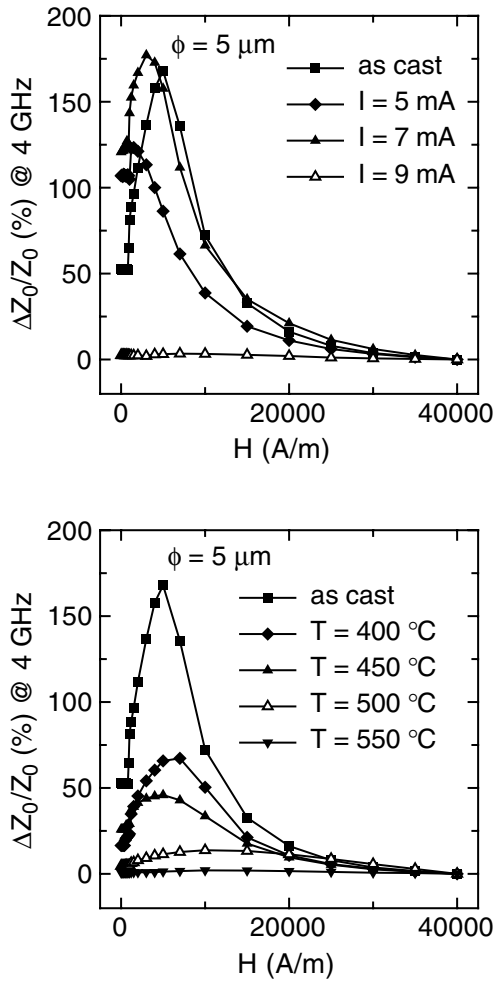

Figure 8. High-frequency GMI curves at a frequency of 4 GHz for as-prepared and annealed thin wires (upper panel: as-prepared and Joule-heated samples; lower panel: as-prepared and furnace-annealed samples).

response for a thick wire is about 150% (Joule heated at 10 mA for 1200 s), while for a thin wire it is about 175% (Joule heated at 7 mA for 1200 s).

Thick and thin samples are affected by thermal treatments in different ways. Thick wires respond to Joule heating with a huge increase of the GMI ratio (figure 7, upper panel) until a current of 10 mA is used to anneal the sample; then, the GMI response lowers and almost vanishes for higher current intensities, even for electrical current values not sufficiently high to start the crystallization process. Furnace-annealed samples show a GMI response that is also improved by thermal treatments, although the increase in performance is not as high as for current-annealed wires. Also, the peak of the GMI curves is much more evident (although not very sharp) for the furnace-annealed samples.

In contrast, thin wires do not seem to be strongly affected by Joule heating until the annealing current is close to the one causing crystallization; under these annealing conditions, the samples show a vanishingly small GMI ratio (figure 8, upper panel). Furnace annealing

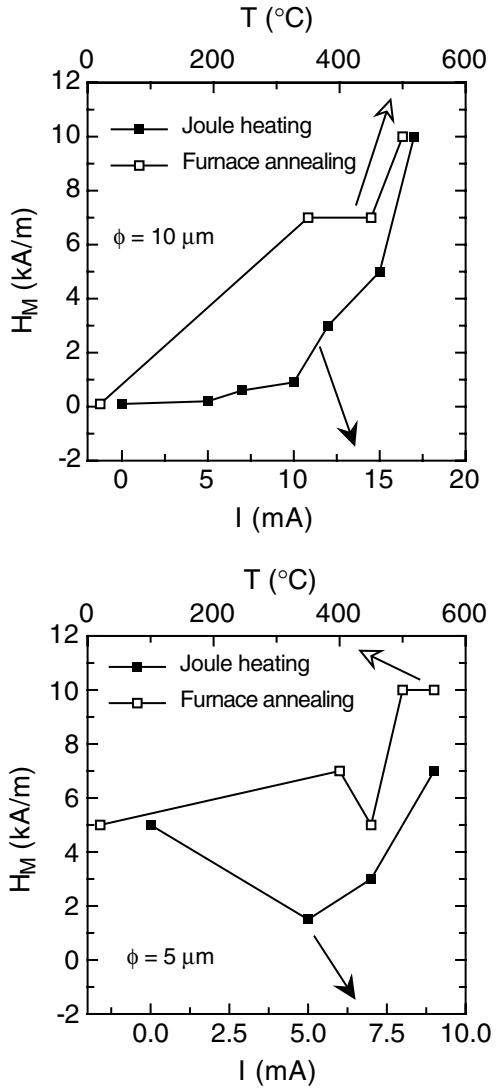

Figure 9. H_M as a function of Joule-heating current or annealing temperature for thick wires (upper panel) and thin wires (lower panel).

influences the GMI response of these thin wires, but is always detrimental to this effect. As for Joule-heated thin wires, crystallized thin samples do not show any GMI effect.

The differences between thick and thin wires and Joule-heated and furnace-annealed samples can also be evidenced by plotting the position of the GMI peak as a function of the thermal treatment; the position of this peak moves towards higher applied field values when the sample is characterized by a higher magnetic anisotropy. The field H_M at which the GMI curves at 4 GHz reach their maximum value is shown in figure 9 as a function of annealing current or temperature. Thick samples start, in the as-prepared state, with a value of H_M equal to zero (figure 9, upper panel): the GMI curve at 4 GHz (the frequency at which the maximum GMI ratio is observed) has a monotonically decreasing shape. Upon annealing, the values of

H_M increase. In agreement with the results obtained for the hysteresis loops, furnace annealing seems even more effective than Joule heating in increasing the value of H_M. However, when the annealing temperature or current becomes close to the one inducing crystallization in the sample, the GMI response approaches zero, Joule-heated and furnace-annealed samples tend to have a similar behaviour and the H_M values become the same. It is worth noting that H_M for Joule-heated thick samples starts increasing significantly for current values $\geqslant 12$ mA; these are also the heating currents that are detrimental to the GMI ratio. Also, comparison with insets of figure 4 confirms the tight link between H_M and H_C: for Joule-heated samples H_M is almost constant (and equal to zero) as long as H_C is vanishingly small; in furnace-annealed wires, H_M and H_C are always larger than their respective values in the as-prepared sample. In summary, for thick wires, Joule heating is effective in improving the GMI response while furnace annealing seems to induce larger anisotropies in the samples; both annealing techniques tend to produce similar results when the annealing induces crystallization and the GMI ratio is strongly reduced.

For thin wires things are different (figure 9, lower panel): H_M has a value much larger than zero in the as-prepared state, and also in this case furnace annealing increases this quantity almost monotonically. In contrast, Joule heating, even if it does not improve the GMI response, lowers the H_M value until the annealing current is sufficiently high to flatten towards zero the GMI curve and H_M starts increasing. However, even for strong annealing processes, Joule heating and furnace annealing do not seem to produce similar results for thin wires. The differences of the H_M value in the as-prepared state between thick and thin samples may be ascribed to the stresses quenched in during preparation that are stronger in thin samples than in thick ones [22]. This difference may be ascribed to the different metallic core diameter–total diameter ratio of the two families of wires: it has been observed that a larger ratio is coupled with lower anisotropies [22]. For these wires too a tight link is observed between H_M and H_C: when the latter is approximately constant (as a function of annealing current or temperature), the former does not change much; both then become larger when samples are submitted to the strongest thermal treatments.

4. Conclusions

A very large GMI variation has been observed at frequencies of a few GHz in Fe-based glass-covered microwires. The different thicknesses of the metallic core (coupled with equal thicknesses of the glass coating) of the two studied families of samples induces different stresses and anisotropies quenched in the as-prepared material; as a consequence, the GMI responses are affected. However, stress relaxations and anisotropy inductions can be obtained by proper thermal treatments. The different expansion coefficients of the metallic core and of the glass coating induce, at the end of the thermal treatment when the temperature decreases, stronger anisotropies in furnace-annealed samples than in Joule-heated wires (where the temperature increases and decreases much faster). These anisotropies, coupled with the relatively large magnetostriction constant of this alloy, contribute to modify the domain structure of the samples and consequently the magnetic permeability directly influencing the GMI response.

Acknowledgments

The authors would like to thank Dr S N Kane for providing the as-prepared samples and Dr F Celegato for helping with some measurements.

References

[1] Panina L V, Mohri K, Bushida K and Noda M 1994 *J. Appl. Phys.* **76** 10
[2] Knobel M and Pirota K R 2002 *J. Magn. Magn. Mater.* **242–245** 33–40
[3] Vazquez M 2001 *J. Magn. Magn. Mater.* **226–230** 693–99
[4] Beach R S and Berkowitz A E 1994 *Appl. Phys. Lett.* **64** 26
[5] Panina L V, Mohri K, Uchiyama T, Noda M and Bushida K 1995 *IEEE Trans. Magn.* **31** 2
[6] Beach R S and Berkowitz A E 1994 *J. Appl. Phys.* **76** 10
[7] Knobel M, Sánchez M L, Gómez-Polo C, Marín P, Vázquez M and Hernando A 1996 *J. Appl. Phys.* **79** 3
[8] Coisson M, Tiberto P, Vinai F and Kane S N 2003 *Sensors Actuators* A **106** 199–203
[9] Da Silva R B, De Andrade A M H, Severino A M, Viegas A D C and Sommer R L 2002 *J. Magn. Magn. Mater.* **249** 288–92
[10] Ménard D, Britel M, Ciureanu P, Yelon A, Paramonov V P, Antonov A S, Rudkowski P and Ström-Olsen J O 1997 *J. Appl. Phys.* **81** 8
[11] Brunetti L, Coisson M, Tiberto P and Vinai F 2002 *J. Magn. Magn. Mater.* **249** 310–14
[12] Coisson M, Tiberto P, Vinai F and Kane S N 2004 *Mat. Sci. Eng.* A **375–77** 1036–39
[13] Dominiguez M, Garcia-Beneytez J M, Vazquez M, Lofland S E and Bhagat S M 2002 *J. Magn. Magn. Mater.* **249** 117–21
[14] Yelon A, Ménard D, Britel M and Ciureanu P 1996 *Appl. Phys. Lett.* **69** 20
[15] Coisson M, Tiberto P, Vinai F and Kane S N 2002 *IEEE Trans. Magn.* **38** 3093–95
[16] Hagiwara M and Inoue A 1993 *Production Techniques of Alloy Wires by Rapid Solidification* ed H H Liebermann (New York: Dekker) p 140
[17] Vazquez M and Zhukov A 1996 *J. Magn. Magn. Mater.* **160** 223
[18] Baranov S A, Berzhanski V N, Zotov S K, Kokoz V L, Larin V S and Torcunov A V 1989 *Phys. Met. Metall.* **67** 70
[19] Rao K V 1983 *Amorphous Metallic Alloys* ed F E Luborsky (London: Butterworth) p 401
[20] Vázquez M, González J and Hernando A 1986 *J. Magn. Magn. Mater.* **53** 323–29
[21] Cullity B D 1972 *Introduction to Magnetic Materials* (Reading, MA: Addison-Wesley) p 227
[22] García K, Zhukov A, Provencio M, Torcunov A, Vázquez M, Kuzminski M, Lachowicz H and Zhukova V 1972 *Proc. Conf. on SMM16* at press
[23] Barandiaran J M and Hernando A 2004 *J. Magn. Magn. Mater.* **268** 309–14
[24] Vázquez M, Gómez-Polo C and Chen D X 1992 *IEEE Trans. Magn.* **28** 3147–9